Direct strength prediction of cold-formed Z-section purlins with support torsion braces combined with span lateral braces

Michael W. Seek[1], Ali Parva[2]

Abstract
The Direct Strength Method is a powerful tool to evaluate the buckling behavior of cold-formed steel structural members. Recent studies have shown that when the Direct Strength method is used in conjunction with analytical procedures that quantify the changes in stress distribution caused by biaxial bending and torsion, the strength of Z-section purlins with one flange attached to sheathing can be accurately predicted. The industry has long assumed a constrained bending stress distribution, but in reality, the distribution of stresses depends on the nature of the external bracing applied. This study investigates the local and distortional buckling strength as predicted by the Direct Strength method for simple span Z-sections with torsion restraints at the support location and combined lateral-torsional braces applied along the length of the purlin. With this bracing configuration, although the lateral displacement of the Z-section is effectively restrained, the Z-section experiences a concentration of stresses at the brace location. As a result of this concentration of stresses, the Z-section may fail at a load level below what is predicted using a constrained bending stress distribution.

An analytical model has been developed that predicts the distribution of stresses in the purlin cross section for systems of purlins with supports torsional braces and paired lateral-torsional braces along the span. The analytical model considers the lateral restraint provided by the flexible diaphragm. Lateral restraints along the span are considered flexible while the span torsion restraints are considered rigid. The model is demonstrated by comparing the predicted strength of several bracing configurations.

1. Introduction

Z-section purlins in roof systems, if left unrestrained, are subject to large lateral and torsion deformations which can substantially reduce the load carrying capacity of the members. The sheathing attached to the top flange of the purlin, provides some lateral and torsional restraint. The restraint provided by through-fastened sheathing systems is relatively stiff and consistent, therefore flexural strength can be accurately predicted. Standing seam systems, on the other hand, have clips that connect the purlin to the sheathing that have either intentional or inherent flexibility. As a result, standing seam systems typically have a much lower diaphragm stiffness

---

[1] Assistant Professor, Old Dominion University, <mseek@odu.edu>
[2] Graduate Research Assistant, Old Dominion University, <aparv001@odu.edu>

than through-fastened systems. Additionally, the lateral and rotational behavior of the clips that provide the connection between purlins is less consistent and can vary widely between manufacturers. As a result, lateral and torsional deformations have a much larger and varied impact on the strength of standing seam systems versus through fastened systems.

In standing seam systems, paired braces symmetric about the mid-span are commonly used to supplement the restraint provided by the sheathing. Most commonly, the braces are placed just inside the third points of the span to reduce the unbraced length of the purlin segment in the middle of the span. Some systems rely on torsion-only braces. Similar to diaphragms or cross frames common in bridge construction, these torsion-only braces are connected between adjacent purlins, as shown in Fig. 1 and prevent adjacent purlins from twisting relative to each other.

There is no continuity of the brace and all resistance to lateral movement is provided by diaphragm action in the sheathing. The advantage of the torsion only bracing system is that the intermediate braces do not require any external anchorage. However, with these torsion-only systems, lateral deflections can exceed limits prescribed by the AISI *Specification*, (AISI, 2012) particularly with flexible diaphragms or steep roofs. To reduce system lateral deflections, torsional braces may be integrated with lateral braces. While lateral deflections are reduced, it can be challenging to anchor these braces externally.
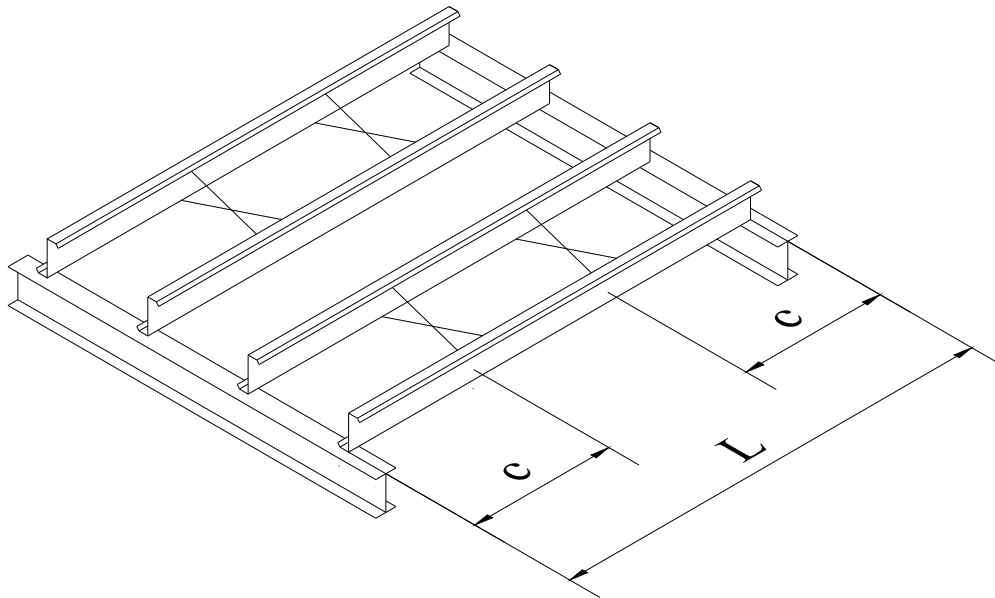
Figure 1: Paired torsion only braces

When designing purlins, there is a disconnect between the supported strength of a purlin and the extent to which it is braced. In the United States, when using the AISI *Specification*,(AISI 2012) to design standing seam roof systems, the test standard AISI S908-13 (AISI 2013), known as the Base Test Method, must be used to determine the nominal moment strength of a purlin for a given span and bracing configuration. This strength is based on the nominal local buckling flexural strength of the cross section, calculated assuming full constrained bending. The strength is then reduced by a reduction factor based on the capacity measured from the base test. The second part of the design, the designer must calculate the forces in the bracing systems, known as anchorage. Anchorage forces are calculated with the understanding that the system deforms and

is not perfectly constrained. When evaluating bracing, the lateral deflection is limited to L/360 for all systems except torsion-only braces which have a limit of L/180.

If a designer does not have Base Test results or is so inclined, he or she may choose to consider a system as discrete braced. In this case, the restraint provided by the sheathing system is ignored and discrete braces that provide lateral and torsional restraint are added along the span of the purlin. Lateral torsional buckling strength is determined assuming the purlin is unrestrained between the brace points. Local and distortional buckling is calculated assuming a constrained bending stress.

Seek et al (2016) has shown that the calculated local and distortional buckling strength of a purlin can be greatly affected by the extent to which it is braced. Therefore, even though the Base Test is intended to represent the bracing configuration used, it is not always appropriate to base the strength of the purlin on the constrained bending stress distribution. The Base Test is conducted on a "flat roof" condition and doesn't account for the changes in biaxial bending introduced on sloped roofs. Furthermore, braces can cause stress concentrations such that local or distortional bucking failures can occur at a brace location as opposed to the mid-span of the purlin where the maximum strong axis moment occurs. Furthermore, displacements measured in the Base Test often exceed the limits allowed by the AISI *Specification*.

The Component Stiffness method (Murray et al. 2009) is used to calculate anchorage forces in purlin supported roof systems. The method, which uses displacement compatibility to determine the distribution of forces throughout the bracing components of a purlin roof system. By superimposing these forces and induced torsional moments, the bending and warping normal stresses can be determined. The method has been applied to simple span purlins with support braces by Seek and Escobales (2016) and simple span systems with torsional braces at 1/3 points by Seek et al (2016).

This method presented in this paper is based on the method presented by Seek et al (2016), but is expanded to apply to lateral-torsional braces applied at any symmetric location along the span. Because the equations are based both on the stiffness of the diaphragm and the lateral stiffness of the braces, by varying the stiffness, the equations provide the full spectrum of possibilities for a purlin with torsion braces - from a system acting as if it has only paired torsion braces to a system that has only discrete braces. Furthermore, by reducing the stiffness of the diaphragm to a negligible value, a system can be analyzed as discrete braced.

2. Calculation of Local and Distortional Buckling Strength

The process to calculate the cross section normal stresses for a simple span purlin system with paired braces that provide either torsion-only or lateral-torsion restraint is provided in the following section. Using displacement compatibility between the purlin and the components resisting lateral and torsional deformation, the forces in those restraining components are determined. By then superimposing these applied loads and the restraining forces of the sheathing and external braces, the bending and warping normal stresses in the purlin can be determined. Equations are provided to determine the stresses at the locations that are typically critical for a simple span system: the purlin mid-span and the brace location. Positive directions for displacements and forces as they act on the purlin are shown in Figure 2.

Figure 2. Positive displacements and forces as they act on purlin

2.1 Lateral Restraint Provided by Diaphragm
The key to the component stiffness method is to determine the force interaction between the purlin and the sheathing. The sheathing provides both lateral restraint, through diaphragm action, and torsional restraint, through the rotational stiffness of the connection between the panel and purlin, k_ϕ. For purlins with torsional braces, the torsional braces are assumed to be infinitely stiff and the rotational stiffness of the sheathing is conservatively ignored. Considering only the horizontal restraint provided by the diaphragm, as a purlin is subject to a uniformly distributed force, w, because of the rotated principal axes, the purlin tries to move laterally. A uniform force, w_{rest}, is developed in the sheathing as it resists this lateral movement. In the absence of interior lateral braces, this uniform force in the diaphragm is calculated

$$w_{rest} = \sigma \cdot w \tag{1}$$

where

$$\sigma = \frac{C_1 \dfrac{\left(\dfrac{I_{xy}}{I_x}\right)L^4}{EI_{my}}}{C_1 \dfrac{L^4}{EI_{my}} + C_2 \dfrac{L^2}{G'spa}} \tag{2}$$

and

$$C_1 = \frac{1}{24} \cdot \left(\frac{c}{L}\right) \cdot \left[1 - 2\left(\frac{c}{L}\right)^2 + \left(\frac{c}{L}\right)^3\right] \tag{3}$$

$$C_2 = \frac{1}{2} \cdot \left(\frac{c}{L}\right) \cdot \left[1 - \left(\frac{c}{L}\right)\right] \tag{4}$$

G' = stiffness of diaphragm (lb/in)
L = Purlin span
spa = width of diaphragm tributary to the purlin (typically purlin spacing)

I_{my} = modified moment of inertia = $\dfrac{I_x I_y - I_{xy}^2}{I_x}$

c = distance from support location to brace location (see Fig. 1)

The above uniform restraint force in the sheathing is determined from displacement compatibility between the purlin and the sheathing. The displacement compatibility assumes that the torsional braces are infinitely stiff, that is, there is no net torsional rotation of the purlin. For an infinitely stiff diaphragm, constrained bending conditions exist and $\sigma \approx I_{xy}/I_x$. As the diaphragm becomes more flexible, lateral deflection will increase and there will be a corresponding reduction in the uniform restraint force.

2,2 Determination of Lateral Brace Force
In the absence of external lateral restraints, the lateral displacement of the purlin at the torsional brace location is

$$\Delta_u = w\left(\frac{I_{xy}}{I_x} - \sigma\right)\frac{C_1 L^4}{E \cdot I_{my}} \tag{5}$$

The force exerted on the system by the external lateral brace, P_L, is determined by enforcing displacement compatibility between the lateral brace and the purlin-diaphragm system based on the displacement of the diaphragm. The force is based on the stiffness of lateral restraint, k_{rest}, relative to the lateral stiffness of the purlin and the diaphragm. The brace force, P_L is calculated from

$$P_L = \Delta_u \cdot \frac{k_{rest}\left(\dfrac{EI_{my}}{C_5 L^3} + \dfrac{G' \cdot spa}{c}\right)}{\dfrac{EI_{my}}{C_5 L^3} + \dfrac{G' \cdot spa}{c} + k_{rest}} \tag{6}$$

where

$$C_5 = \frac{1}{2}\left(\frac{c}{L}\right)^2 - \frac{2}{3}\left(\frac{c}{L}\right)^3 \tag{7}$$

2.3 Distribution of Lateral Brace Force
The brace force is partially distributed to the diaphragm and partially distributed to the purlin according to the relative stiffness of each component. Much of the force is transferred directly to the diaphragm at the brace location however, some of the force is transferred uniformly along the span. The lateral forces acting on the diaphragm through interaction with the purlin are shown in Fig. 3. The uniformly distributed force is first determined by enforcing displacement compatibility between the purlin and diaphragm for the portion of the span between the support point and brace location. The uniform force generated between the purlin and the sheathing as a result of the brace force is

5

$$w_d = \frac{P_L}{c} \left(\frac{\dfrac{EI_{my}}{C_5 L^3}}{\dfrac{EI_{my}}{C_5 L^3} + \dfrac{G' \cdot spa}{c}} \right) \frac{\left(\dfrac{24}{5}\right) \dfrac{8G' \cdot spa}{c^2}}{\dfrac{384 EI_{my}}{5c^4} + \dfrac{8G' \cdot spa}{c^2}} \tag{8}$$

This force acts in a direction opposite to the uniform force in the diaphragm, w_{rest} so the net uniform force in the diaphragm is $w_{rest} - w_d$. The remainder of the total brace force is transferred to the diaphragm at the brace location. This concentrated force between the purlin and diaphragm, P_d is

$$P_d = \frac{\dfrac{G' \cdot spa}{c}}{\dfrac{EI_{my}}{C_5 L^3} + \dfrac{G' \cdot spa}{c}} \left[P_L - w_d \frac{\left(\dfrac{G' \cdot spa}{C_2 L^2} + \dfrac{EI_{my}}{C_1 L^4}\right)\left(\dfrac{EI_{my}}{C_5 L^3}\right)}{\left(\dfrac{EI_{my}}{C_1 L^4}\right)\left(\dfrac{G' \cdot spa}{C_2 L^2}\right)} \right] \tag{9}$$

The remaining portion of the brace force that is resisted by the purlin through flexure, P_p is

$$P_p = P_L - P_d \tag{10}$$

The total brace force, P_L, is subdivided into the two forces because the portion of the force resisted by the purlin, P_p, causes weak axis bending stresses, while the portion of the force resisted by the diaphragm results in a concentrated torque that must be resisted by the torsion brace.
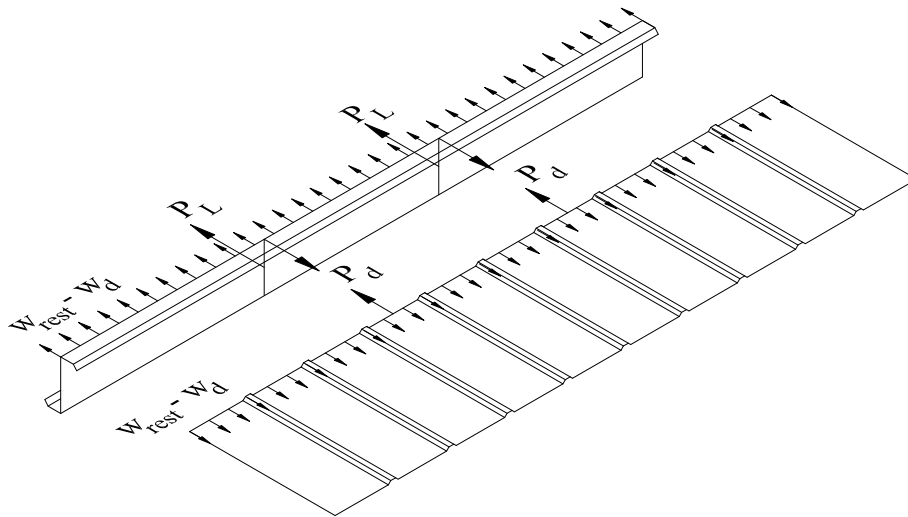
Figure 3 Lateral forces interacting between purlin and diaphragm

With the application of the brace, the net lateral deflection of the purlin at the brace location is

$$\Delta_{rest} = P_L \cdot k_{rest}$$

The lateral displacement also needs to be investigated at the mid-span of the purlin as there is additional displacement of the purlin relative to the brace. The mid-span lateral displacement of the purlin, Δ_{mid}, including the effects of the lateral restraint is

$$\Delta_{mid} = \left[w\left(\frac{I_{xy}}{I_x} - \sigma\right) + w_d \right] \frac{5L^4}{384E \cdot I_{my}} - \frac{P_p c}{24E \cdot I_{my}}\left(3L^2 - 4c^2\right) \tag{11}$$

Naturally, both the net deflection of the purlin at the brace, and the mid-span lateral deflection should be less than the unrestrained displacement of the diaphragm. It is important to quantify the lateral deflection of the purlin because second order torsion effects are approximated from the displacement.

2.4 Torsional Moments
The purlin is subject to a uniform torque along its length as a result of the eccentricity of applied force relative to the web of the purlin, e_{sx}, and the eccentricity of the uniform lateral restraint applied by the sheathing at an eccentricity of e_{sy}. The uniform torque along the length of the purlin from first order effects is

$$t_{1st} = (w)\left(\sigma \cdot e_{sy} - e_{sx}\right) - w_d e_{sy} \tag{12}$$

Similarly, torsion is induced as the mid-span of the purlin deflects laterally relative to the supports. The torsion is approximated to have a parabolic distribution where the peak torsion at mid-span, t_{2nd} is

$$t_{2nd} = -w \cdot \Delta_{mid} \tag{13}$$

The torsion introduced along the length of the purlin is balanced at the torsion brace locations. Because purlin torsion behavior is dominated by warping torsion, the balance of torsion ignores the minimal contribution of pure torsion, which greatly simplifies the equations and results in negligible difference in the calculated results. First and second order torsion is separated such that relative magnitudes can be evaluated. The brace torque from first order torsion is

$$T_{1st} = -C_3 t_{1st} L \tag{14}$$

where

$$C_3 = \frac{1}{4} \cdot \frac{1 - 2\left(\dfrac{c}{L}\right)^2 + \left(\dfrac{c}{L}\right)^3}{3\left(\dfrac{c}{L}\right) - 4\left(\dfrac{c}{L}\right)^2} \tag{15}$$

The brace torque from the second order effects that are approximated with a parabolic load distribution is

$$T_{2nd} = -C_4 t_{2nd} L \tag{16}$$

where

$$C_4 = \frac{1}{15} \cdot \frac{3 - 5\left(\frac{c}{L}\right)^2 + 3\left(\frac{c}{L}\right)^4 - \left(\frac{c}{L}\right)^5}{3\left(\frac{c}{L}\right) - 4\left(\frac{c}{L}\right)^2} \qquad (17)$$

The torsion braces resist additional torque that results from the eccentricity between the lateral brace, P_L, and the concentrated force transferred to the diaphragm. P_d. Because these forces are transferred through the purlin at the brace location, they do not induce additional warping stresses into the purlin. In most torsional brace systems, the lateral brace is located at the centroid of the purlin, however, the brace may have an eccentricity, e_b as shown in Fig. 4.
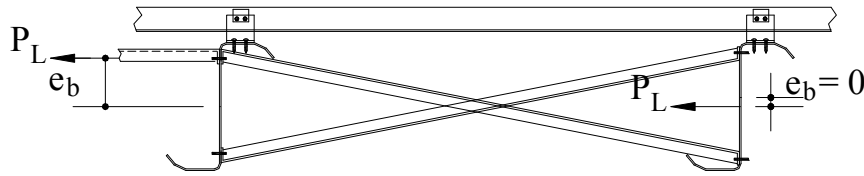
Figure 4 Eccentricity of lateral brace

The total torque transferred between the brace and the purlin at each brace location, T_b, is

$$T_b = T_{1st} + T_{2nd} + P_d e_{sy} - P_L \cdot e_b \qquad (18)$$

In Eq. 18, the sign of the brace torque, T_b, is in the direction in which it acts on the purlin. To balance the moment introduced to the torsion brace at purlin, a shear force, V_i, is applied to each purlin, where

$$V_i = d_i \frac{\Sigma(T_b)_i}{\Sigma(d_i)^2} \qquad (19)$$

This assumes that the lateral-torsional brace member is continuous through the purlins. The distance, d_i is measured from the center of rigidity of the system of purlins connected by the brace. In Eq. 19, the distance, d_i, is positive if in the upslope direction and negative if in the downslope direction. If the purlins are have nominally equal cross sections, loading, and spacing, the center of rigidity is the geometric center of the line of purlins.
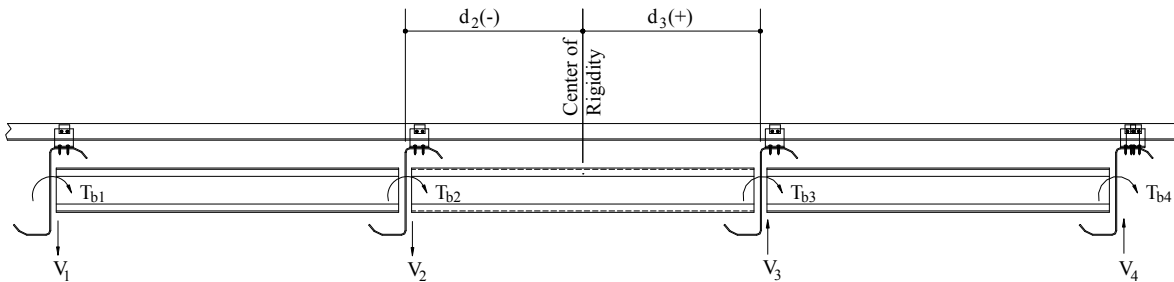
Figure 5 Balance of moment and shear in braces

2.5 Bending and Warping Normal Stresses

Biaxial Bending and Warping normal stresses can now be calculated by superposition of the forces and moments acting on the purlin. The two critical locations to determine stresses are the mid-span of the purlin and at the brace location.

The total mid-span moment, M_{mid}, about the orthogonal x-axis from combined first order and second order forces is

$$M_{mid} = \frac{w(\cos\theta)L^2}{8} + (V_i)c$$
(20)

At the brace location, the bending moment about the orthogonal x-axis, M_c is

$$M_c = w(\cos\theta)\frac{c}{2}((L-c)+(V_i)c$$
(21)

The bending normal stresses from biaxial bending of the cross section are calculated at each point along the cross section defined by coordinates (x,y) by

$$f_b = \left(\frac{wL^2}{8}+V_i\cdot c\right)\left[\frac{-y}{I_{mx}}+\frac{x\dfrac{I_{xy}}{I_x}}{I_{my}}-\frac{x\cdot\sigma}{I_{my}}+\frac{y\dfrac{I_{xy}}{I_y}\sigma}{I_{mx}}\right]+\left(P_p\cdot c-\frac{w_dL^2}{8}\right)\left[-\frac{x}{I_{my}}+\frac{y\dfrac{I_{xy}}{I_y}}{I_{mx}}\right]$$
(22)

At the Brace location

$$f_b = \left(w\frac{c}{2}(L-c)+V_i\cdot c\right)\left[\frac{-y}{I_{mx}}+\frac{x\dfrac{I_{xy}}{I_x}}{I_{my}}-\frac{x\cdot\sigma}{I_{my}}+\frac{y\dfrac{I_{xy}}{I_y}\sigma}{I_{mx}}\right]+\left(P_p\cdot c-w_d\frac{c}{2}(L-c)\right)\left[-\frac{x}{I_{my}}+\frac{y\dfrac{I_{xy}}{I_y}}{I_{mx}}\right]$$
(23)

Warping torsion normal stresses are calculated according to the AISC Torsion Analysis Design Guide (Seaburg and Carter, 1997). The general equation for warping torsion normal stresses, f_w, is

$$f_w = E\cdot W_N \cdot \phi''$$
(24)

where W_N is the normalized warping function at a specific point on the cross section and $\phi``$ is the second derivative of the rotation function for the applied load with respect to the z-axis along the span of the beam. Normalized warping functions, W_N, can be determined using the numerical methods outlined by Yu and Laboube (2010). Rotation functions are derived for each torsion function the purlin is subjected to (uniform distribution, parabolic distribution, paired concentrated torque) at each of the locations to be investigated (mid-span and the brace location.

At the mid-span location, the rotation functions are:

9

Uniform Torsion

$$\phi_u" = \frac{t_{1st}}{GJ}\left(\frac{1}{\cosh\left(\dfrac{L}{2a}\right)} - 1\right) \tag{25}$$

Parabolic Torsion

$$\phi_p" = \frac{t_{2nd}}{GJ}\left[\frac{8a^2}{L^2}\left(1 - \frac{1}{\cosh\left(\dfrac{L}{2a}\right)}\right) - 1\right] \tag{26}$$

Concentrated Torsion at Brace Location

$$\phi_{brace}" = \frac{T_{1st}+T_{2nd}}{GJ}\left(\frac{1}{a}\right)\left[\sinh\left(\frac{L}{2a}\right)\left(\frac{\sinh\left(\dfrac{c}{a}\right)+\sinh\left(\dfrac{L\text{-}c}{a}\right)}{\tanh\left(\dfrac{L}{a}\right)} - \cosh\left(\frac{L\text{-}c}{a}\right)\right) - \cosh\left(\frac{L}{2a}\right)\sinh\left(\frac{c}{a}\right)\right] \tag{27}$$

At the brace location, the rotation functions are:

Uniform Torsion

$$\phi_u" = \frac{t_{1st}}{GJ}\left(\cosh\left(\frac{c}{a}\right) - \tanh\left(\frac{L}{2a}\right)\sinh\left(\frac{c}{a}\right) - 1\right) \tag{29}$$

Parabolic Torsion

$$\phi_p" = \frac{t_{2nd}}{GJ}\left[\frac{8a^2}{L^2}\left(\frac{\cosh\left(\dfrac{L}{a}\right)-1}{\sinh\left(\dfrac{L}{a}\right)}\sinh\left(\frac{c}{a}\right) - \cosh\left(\frac{c}{a}\right) + 1\right) + 4\left(\frac{c}{L}\right)^2 - 4\left(\frac{c}{L}\right)\right] \tag{30}$$

Concentrated Torsion at Brace Location

$$\phi_{brace}" = \frac{T_{1st}+T_{2nd}}{GJ}\left(\frac{1}{a}\right)\sinh\left(\frac{c}{a}\right)\left(\frac{\sinh\left(\dfrac{c}{a}\right)+\sinh\left(\dfrac{L\text{-}c}{a}\right)}{\tanh\left(\dfrac{L}{a}\right)} - \cosh\left(\frac{L\text{-}c}{a}\right) - \cosh\left(\frac{c}{a}\right)\right) \tag{31}$$

Combining the three rotation functions for each of the torsion distributions, the net normal stress from warping torsion in calculated by Eq. 28.

$$f_w = E \cdot W_N \cdot \left(\phi_u" + \phi_p" + \phi_{3rd}"\right) \tag{28}$$

2.6 Direct Strength Method to Determine Local and Distortional Buckling Strength
The normal stresses from bending and torsion are combined at each location at the cross section. The location of peak stress in the cross section is located and the stresses in the cross section are

10

scaled to the point of first yield by the factor $F_y/(f_b+f_w)$. The yield moment of the cross section, M_y, then is determined by multiplying the scale factor by the strong axis moment at either the mid-point, M_{mid}, or the brace location, M_{brace}, depending on which point along the span is to be evaluated.

With the stresses in the cross section scaled, a finite strip buckling analysis is performed using CUFSM v4.03 (Li and Schafer, 2010) to determine the critical local and distortional buckling moments, $M_{cr\ell}$, and M_{crd}, respectively. Using the provisions Appendix 1 of the 2012 AISI *Specification* (AISI, 2012), the nominal local buckling strength is determined according to Section 1.2.2.1.2 with $M_{ne} = M_y$ and the nominal distortional buckling strength is determined according to Section 1.2.2.1.3. The minimum of the local buckling strength and the distortional buckling strength is considered to be the design strength.

In this analysis, lateral torsional buckling has not been considered. Failure modes in tests of torsion braced purlins (Emde, 2010) cite the dominant failure modes as local buckling and distortional buckling. The lateral torsional buckling strength is complicated by the lateral and torsional restraint provided by the sheathing over the unbraced length between the brace locations. Additional research is needed to evaluate the resistance of purlin systems to lateral torsional buckling to confirm that it does not control as the predicted failure mode.

It should be noted that the determination of the yield moment is dependent upon the distribution of stresses in the cross section. As the method presented approximates second order effects, it is expected that the distribution of stresses will change with increasing load levels. This change in stresses does have a small impact on the predicted nominal strength of the purlin. However, for systems with torsion braces, those second order effects are minimal and the predicted nominal strength will only change slightly. Therefore, as long as the applied load level is reasonably close to the ultimate load the purlin can support, the nominal strength can be reasonably predicted. To find this ultimate load, no more than is single iteration is likely required.

3. Example Comparisons
To demonstrate the capabilities of the method, several bracing configurations are compared. First, a system with torsion-only braces is compared to the results of a base test to show the correlation of the method to test. Next, flexible lateral braces are added to the torsion-only case to demonstrate the impact the addition of the lateral restraints has on the strength of the purlin. Finally, the system with paired lateral-torsion restraints is modified with the lateral brace relocated to the mid-span of the purlin to demonstrate the impact brace location has on the flexural strength.

3.1 Analysis Parameters
Seek et al. (2016) showed, using a similar displacement compatibility approach to determine the cross section stresses, that the flexural capacity of Z-sections with paired torsion braces could be accurately predicted. The local and distortional buckling strength of several Z-sections was calculated and compared to the results of a series of base tests performed by Emde (2010). In the series, twelve tests were performed with three of each cross section: 8ZS2.00x057, 8ZS2.00x100, 10ZS2.00x057 and 10ZS2.00x100. For both the 8ZS2.00x100 and 10ZS2.00x100 tests, large lateral force demands were placed on the diaphragm with lateral deflections on the

order of L/60. As such large lateral deflections can be undesirable, lateral braces may be applied to reduce the deflections.

Using the tests of the 8ZS2.00x100 purlins as a reference point, the impacts on the local and distortional buckling strength with additional lateral braces are investigated. Seek et al. (2016) showed that the base test configuration itself introduces several second order effects. The equations provided herein are intended to apply to "real" systems and therefore have eliminated some of those second order effects.

The system evaluated utilizes an 8ZS2.00x0.100 purlin with the measured yield stress, Fy = 79.1 ksi, and calculated section properties shown in Table 1. The purlin span, L=27 feet. The spacing of the purlins and correspondingly, the depth of diaphragm tributary to each purlin, spa, is 5 feet. The standing seam diaphragm stiffness, G' = 110 lb/in., and the depth of diaphragm tributary to each purlin, spa = 5 feet. The effective standoff of the diaphragm is approximated as 2.5 in. in accordance with Seek and McLaughlin (2017). Lateral-torsional braces are applied in a two purlin configuration such that the shear forces generated in the braces are balanced between the adjacent purlins. When used, the stiffness of the lateral brace is 4 kip/in/purlin and the torsion braces are approximated to be infinitely stiff.

Table 1: Calculated Properties

Cross Section	I_x (in^4)	I_y (in^4)	I_{xy} (in^4)	I_{my} (in^4)	I_{mx} (in^4)	J (in^4)	C_w (in^6)
8ZS2.00x0.100	14.191	2.2746	4.1445	1.064	6.639	4.810×10^{-3}	26.402

It should be noted that comparisons between tests and analytical models are made based on the supported uniform load of the purlin as opposed to the ultimate moment. The ultimate moment in the purlin is affected by the shear forces caused by the torsional braces which, accordingly are affected by a number of variables within the system of purlins. Therefore, to make a valid comparison between systems, it is most meaningful to look at the uniform load supported. When comparing relative displacements and forces within a system, comparisons are made using a uniformly distributed load of 150 lb/ft. When comparing the ultimate capacity of a system of purlins, the ultimate uniform load that can be supported before failure is reported.

3.2 System with Torsion Only Braces
To validate the presented method and provide a reference point to compare the impacts of adding lateral braces, the predicted strength of a torsion-only system is compared to a base test performed by Emde (2010). Emde performed three tests on 8ZS2.00x0.100 purlins and the first test from the series is used for comparison in this study. In the test, the torsion only-braces were located at a distance c =10.5 feet from the ends of the purlin and the purlins supported a pressure of 37.65 psf which translated into a supported uniform load including dead weight of 152.4 plf.

The system was first evaluated using the second order effects applicable to the Base Test Method as outlined by Seek et al (2016) with the exception that braces were modeled at the actual location as opposed to the third points as approximated by Seek. The analytical model predicts that the purlin will fail at a supported uniform load of 156.5 plf versus the tested uniform load of 152.3 plf. The predicted mode of failure is distortional buckling at the brace location of the downhill purlin. Although the exact failure mode of each test was not reported by Emde, local or

distortional buckling at the brace location was reported as one of the most common failure modes. It should be noted that the system underwent large lateral deflections (6.07 in. measured and 5.97 in. calculated) and subsequently experienced large second order effects.

The torsion-only brace configuration was then analyzed as a "real" system, or in other words, the system was evaluated by eliminating the second order effects inherent in the base test as presented in this paper. It should be noted, to use the equations presented in this paper for a torsion-only brace system, the stiffness of the lateral restraint, k_{rest}, must be reduced to zero. For this system, the tributary depth of the diaphragm is the purlin spacing (5 feet) as opposed to 3 feet 6 in. from the base test. With a greater depth of diaphragm tributary to the purlin, the lateral diaphragm deflection is correspondingly reduced.   The calculated lateral deflection of the purlin/diaphragm at mid-span is 5.09 in. As expected, with reduced diaphragm deflection and without the second order effects inherent in the base test, the predicted capacity of the purlin in the "real" system increases slightly to 162 plf relative to the base test (156.5 plf predicted). Similarly as the second order torsion demands are reduced for the "real" system, the resisting moment at the torsion brace is reduced. A summary comparison is provided in Table 2.

Table 2: Comparison of Torsion-only Braced Systems

Bracing Configuration	Ultimate load, w (plf)	Δ_{mid} at w = 150 plf (in.)	T_b at w = 150 plf (lb-in.)
Torsion-only - Base Test (Tested)	152.4	6.07	-
Torsion-only –Base Test (Predicted)	156.5	5.97	6430
Torsion-only – (Real system)	162.3	5.09	4685

The typical distribution of stresses across the cross section are shown for the mid-span in Fig. 5(a) and at the brace location in Fig. 6(b). Because of the large lateral deflections, the purlin is effectively subjected to a large biaxial bending force. For the mid-span location, the peak stress occurs at the intersection between the flange and the web and drops significantly moving towards the flange tip.   Similarly, at the brace location, the peak stress occurs at the flange-web intersection, but the addition of the large concentrated torque at the brace causes an increase in the stresses towards the flange tips. As a result of this different distribution of stresses, although the magnitude of the net stress in the cross section is less at the brace location, the critical distortional buckling moment may control at the brace location as it did for the particular configuration investigated.

The diaphragm provides all the lateral resistance and as a result, large shear forces may accumulate in the diaphragm at the end of the span. For the configuration investigated, the maximum unit shear in the diaphragm at the end of the span is 82.2 lb/ft.

13

| (a) Mid-span | (b) Brace Location |
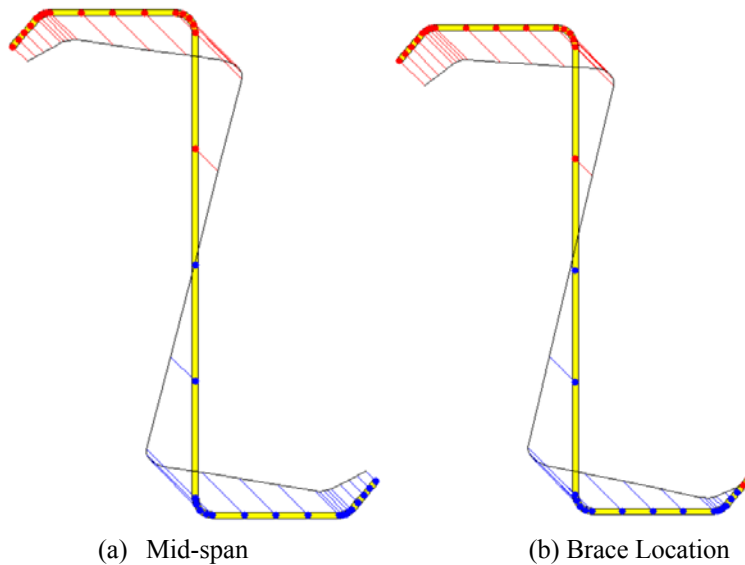
Figure 6 Stress distributions for paired torsion braces

3.3 System with paired lateral-torsion braces

For comparison, the next system evaluated has the same configuration as the previous torsion-only system, but with additional lateral restraint applied at the torsion brace location. The stiffness of the restraint tributary to a single purlin is 4 kip/in., which is a fairly stiff restraint for purlin systems. With the additional lateral restraint applied, the predicted uniform load capacity of the purlin increases to 188.7 lb/ft. At that ultimate load, the failure is predicted to occur at either the mid-span or the brace location.

Naturally, with the applied lateral brace, the lateral deflection along the span will be greatly reduced. When subjected to a uniformly distributed load of 150 lb/ft, the lateral deflection of the purlin at the brace location is 0.091 in. There is additional lateral deflection of the purlin between the braces and the maximum lateral deflection at mid-span is (0.225 in.).

The distribution of stresses across the cross section are shown for the mid-span location in Fig. 7 (a) and the brace location in Fig. 7 (b). At the mid-span location, as a result of the reduced lateral deflection, the distribution of stresses closely resembles the constrained bending condition. The peak stress occurs at the web-flange intersection. At the brace location, however, the peak stress shifts to the flange-stiffener intersection as a result of the concentrated force applied by the lateral brace. This behavior is similar to a multi-span beam that experiences negative moment at an interior support location. The ultimate supported load is controlled by the distortional buckling strength which is predicted to occur at the same load level at either the mid-span or the brace location. Although the overall stresses are higher at the mid-span location, the change in stress distribution at the brace location lowers the critical buckling moment at the brace location.

Shear demands on the diaphragm are greatly reduced as a result of the added lateral restraint. The maximum unit shear in the diaphragm at the end of the span is 19.7 lb/ft. The total lateral brace force that is generated at each brace, P_L, is 365 lb. Of that total brace force, 122 lb is

transferred through to the diaphragm as P_d and the remaining force, $P_p = 243$ lb, is resisted in weak axis flexure by the purlin.

(b) Mid-span   (b) Brace Location
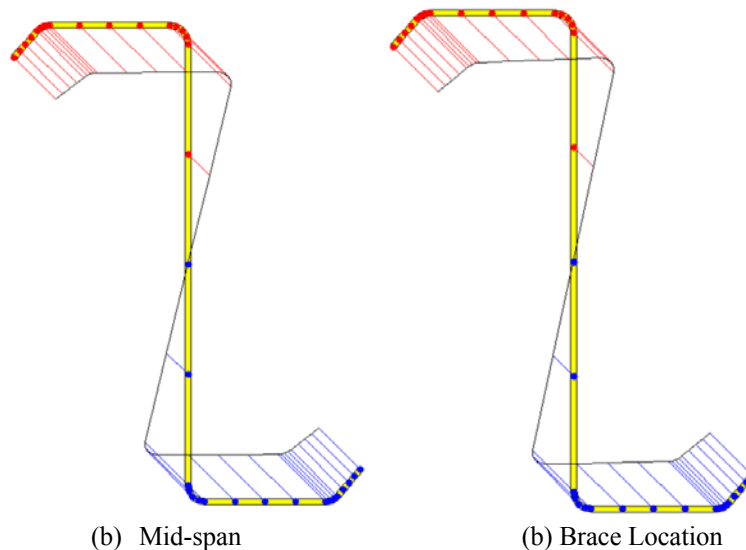
Figure 7 Stress distributions for paired combined lateral-torsion braces

3.4 System with midpoint lateral brace
A midpoint lateral brace can be modeled by locating the brace at mid-span, $c = L/2$. In this configuration, the lateral brace force, P_L, and the moment resisted by the brace should be doubled for the single point brace. Similarly, to match the net brace lateral stiffness of the previous analytical model, the stiffness of the brace is halved such that $k_{rest} = 2$ kip/in.

The distribution of stresses in the cross section are shown in Figure 8. Similar to the previous lateral torsion brace, the lateral force at the brace location has the results in a large weak axis moment that shifts in peak stresses towards the flange tips. Because this large weak axis moment occurs at the location of maximum strong axis moment, there is a reduction on the supported load. The ultimate uniform load for the mid-point brace is 160.1 lb/ft. This supported load represents a substantial reduction (18%) when compared to the paired lateral-torsion braces located a short distance (3 feet) away from the mid-span.

The supported uniform load capacity of the mid-point brace configuration is comparable to the paired torsion only braces. It has long been understood within the industry that midpoint restraints can reduce the supported capacity of a purlin system relative to a system that just has supports restraints (a configuration similar to torsion-only braces). Much of this experience and understanding has been realized through proprietary testing. The authors have not yet found a published set of tests with which to provide a comparison of predicted strength to tested strength for the presented method. However, although the comparison provided herein is anecdotal, it supports this trend and provides a valid reasoning for the reduction in strength for a mid-point lateral brace. A comparison of the relative stresses and ultimate uniform load for each of the bracing configurations is provided in Table 3.

15
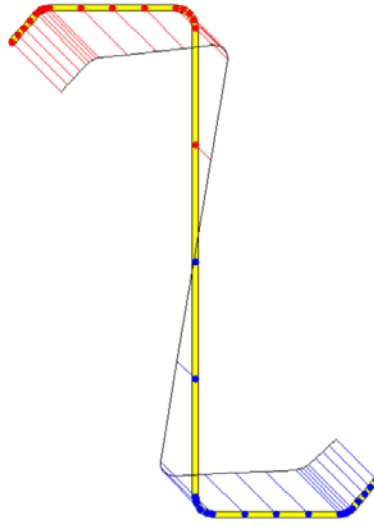
Figure 8 Stress distribution for mid-span lateral-torsion brace

The force demands on the external braces for a mid-span lateral-torsion brace are comparable to those of braces paired along the span. When using the methodology presented in this paper for a mid-span brace configuration, the equations should be approached as if there are two braces meeting at the midpoint. The lateral stiffness of each of these restraint, k_{rest}, should be half the total stiffness of the brace, and the lateral force, P_L, and the moment, M_b should be doubled. The forces generated in each of the restraining components of the system are summarized in Table 4 for each bracing configuration.

Table 3: Failure Modes and Stresses

Bracing Configuration	Ultimate load, w (plf)	Controlling Strength	Controlling Location	Peak stress location	$f_b + f_w$ at w = 150 plf (ksi)	$F_y / (f_b + f_w)$
Torsion-only – (c/L=0.39)	162.3	Distortional Buckling	Brace	Web-flange Juncture (Tens.)	64.87	1.219
Paired Lateral-Torsion (c/L=0.39)	188.7	Distortional Buckling	Mid-span / Brace	Flange-stiffener junction (Comp.)	47.86	1.653
Midpoint Lateral-Torsion (c/L=0.5)	160.1	Distortional Buckling	Mid-span = Brace	Flange-stiffener junction (Comp.)	56.91	1.390

Table 4: System deformations and force demands of restraining components

Bracing Configuration	Ultimate Load, w (plf)	Δ_{mid} at w = 150 plf (in.)	M_b at w = 150 plf (lb-ft)	P_L at w = 150 plf (lb)	Diaphragm max unit shear (lb/ft)
Torsion-only – (c/L=0.39)	162.3	5.09	4685	0	82.2
Paired Lateral-Torsion (c/L=0.39)	188.7	.225	1151	365.5	19.7
Midpoint Lateral-Torsion (c/L=0.5)	160.1	.154	2134	616.8	26.5

A final comparison is provided in Table 5 relating the ultimate load of each bracing configuration to the ultimate load based on constrained bending. The constrained bending strength was calculated from the Direct Strength Method. For the constrained bending case, distortional buckling controlled the strength. Traditionally, when purlin systems are evaluated by the base test, the tested strength is compared to the local buckling strength of the purlin. For

the purlin investigated, the local buckling strength is 99% of the yield moment strength, whereas the distortional buckling strength is 76% of the yield moment strength. From the comparison in Table 5, it is apparent that the deviations from the constrained bending strength can vary widely based on the bracing configuration.

Table 5: Failure modes and strength Reduction Relative to Constrained Bending

Bracing Configuration	Supported Load at Failure (plf)	Controlling Buckling Strength	Reduction Relative to Constrained Bending
Constrained Bending	193.1	Distortional–Mid-span	1.00
Torsion-only - Base Test (Tested)	152.4	(not reported)	0.79
Torsion-only –Base Test (Predicted)	156.5	Distortional – Brace	0.81
Torsion-only – (Real system)	162.3	Distortional - Brace	0.84
Paired Lateral-Torsion (c/L=0.39)	188.7	Distortional Mid/Brace	0.98
Midpoint Lateral-Torsion (c/L=0.5)	160.1	Distortional Mid/Brace	0.83

It is possible to use the presented method to calculate the stresses of a discretely braced purlin, that is, a purlin that does not have additional diaphragm restraint at the top flange. In the equations, the stiffness of the diaphragm, G', should be set to a negligible value (1 lb/in. for example). It cannot be set to zero, because as the equations are configured, this will result in the division by zero. If the purlin is attached to any system that provides diaphragm restraint, it is advisable that the diaphragm be included. If the stiffness of the diaphragm it is not known, underestimating the stiffness of the diaphragm will result in a conservative approximation of the strength.

4. Conclusions

A method is provided to calculate the local and distortional buckling strength for a simple span purlin with one flange attached to sheathing and braced by torsion-only or lateral-torsion braces at symmetrically paired locations along the span. Using displacement compatibility, the interaction between the purlin and the restraint provided by the diaphragm and braces is quantified. By superimposing these bracing forces on the applied forces, the biaxial bending and warping torsion normal stresses across the cross section are determined. With this stress distribution, a finite strip buckling analysis is performed to determine the critical local and distortional buckling moments.

The presented method is compared to base test results for a purlin system with torsion-only braces and shows good correlation. The method is next applied to a purlin in "real" system that is not subject to the second order effects inherent in the base test method and shows a slight increase in capacity. Comparisons are then made to systems with lateral restraint in addition to the torsion restraints. For paired torsion braces with braces located just inside the third points of the span, the strength of the system was close to the constrained bending strength. For lateral-torsion braces applied at the mid-span, the strength was reduced to the level of the torsion-only braces, validating the known but not well understood trend of the reduced strength of mid-point restrained purlins.

The presented method allows the user to predict the impact that the level of restraint provided by the diaphragm and external braces have on the strength of a purlin system with one flange attached to sheathing. Additional comparison to tests or finite element models is required, particularly for combined lateral-torsion systems, to validate the method. Additionally, for the

method to be truly useful for design, it needs to be expanded to from single span systems to apply to the continuous purlin systems on sloped roofs.

Acknowledgments

References

AISI (American Iron and Steel Institute). (2013) S908-13 Base Test Method for Purlins Supporting a Standing Seam Roof System. Washington, DC.

AISI (American Iron and Steel Institute). (2012). North American Specification for the Design of Cold-Formed Steel Structural Members. Washington, DC.

Seaburg, P. A., Carter, C. J. (1997). *Steel Design Guide Series 9: Torsional Analysis of Structural Steel Members.* American Institute of Steel Construction. Chicago, IL.

Emde, M. G. (2010) *Investigation of Torsional Bracing off Cold-Formed Steel Roofing Systems.* Master's Thesis. University of Oklahoma. Norman, OK.

Li, A., Schafer, B.W. (2010) "Buckling analysis of cold-formed steel members with general boundary conditions using CUFSM: conventional and constrained finite strip methods." Proceedings of the 20th International Specialty Conference on Cold-Formed Steel Structures.

Murray, T. M., Sears, J., and Seek, M. W. (2009). *D111-09 Design Guide for Cold-Formed Steel Purlin Roof Framing Systems*. American Iron and Steel Institute. Washington, DC.

Seek, M. W. (2014). "Improvements to the prediction of brace forces in Z- purlin roof systems with support + third point torsion bracing". Proceedings of the 22nd International Specialty Conference on Cold-Formed Steel Structures.

Seek, M. and Escobales, N. (2016). "Computational Procedure for Normal Stresses in C-Sections and Z-Sections with One Flange Attached to Sheathing." *Journal of Structural Engineering*. ASCE. 142 (2).

Seek, M.W., and McLaughlin, D. (2017) "Impact of clip connection and insulation thickness on bracing of purlins in standing seam roof systems." Conference Proceedings, SSRC Annual Stability Conference. Structural Stability Research Council, University of Missouri-Rolla, Rolla, Missouri.

Seek, M.W., Ramseyer, C. and Kaplan, I. (2016) "A Combined Direct Analysis and Direct Strength Approach to Predict the Flexural Strength of Z-Purlins with Paired Torsion Braces". Proceedings of the 23rd International Specialty Conference on Cold-Formed Steel Structures.

Yu, W. and R. A. Laboube. (2010) *Cold-Formed Steel Design, 4th ed.* John Wiley & Sons. Hoboken, NJ.

Zetlin, L and G. Winter (1955), "Unsymmetrical Bending of Beams with and without Lateral Bracing." *Journal of the Structural Division*, ASCE, Vol. 81, 1955.